Iraqi Journal of Science, 2017, Vol. 58, No.2B, pp: 961-970
DOI:10.24996.ijs.2017.58.2B.20

ISSN: 0067-2904

Methods and Simulations used to Detect Photons from Exoplanets of a Parent Star

Ali Talib[1], A. D'Onofrio[2] , F. Terrasi[2]

[1]Department of Astronomy, College of Science, University of Baghdad, Bghdad, Iraq.
[2]Department of Mathematics and Physics, Second University of Naples, Italy.

Abstract

The extrasolar planets in the vicinity of stars are expected to be bright enough and are very difficult to be observed by direct detection. The problem is attributed to the side loops of the star that created due to the telescope diffraction processing. Several methods have been suggested in the literatures are being capable to detect exoplanet at a separation angle of $4\lambda/D$ and at a contrast ratio of 10^{-10}. These methods are more than one parameter function and imposing limitations on the inner working distance. New simple method based on a circular aperture combined with a third power Gaussian function is suggested. The parameters of this function are then optimized based on obtaining a minimum inner working distance This method is capable of detecting exoplanet with an angular separation of $4\lambda/D$ and a contrast ratio of 10^{-10} and it is much easier to be implemented practically.

Keywords: Mathematical modeling, optical imaging, Fourier optics, resolution, exoplanets detection.

الطرق والمحاكاة المستخدمة لتحسس الفوتونات من الكواكب الخارجية حول النجم

علي طالب[*1]، انتونيو دونوفريو[2] ، فيليبو تراسي[2]

[1]قسم الفلك والفضاء، كلية العلوم، جامعة بغداد، بغداد، العراق.
[2]قسم الرياضيات والفيزياء، جامعة نابولي الثانيه، ايطاليا

الخلاصة

ان الكواكب الخارجية بالقرب من المناطق المجاورة للنجوم المضيئة من الصعوبة رصدها بالطرق المباشرة. ان المشكلة تكمن في الاطراف الجانبية التي تظهر نتيجة عملية الحيود خلال رصد النجوم بواسطة التلسكوبات البصرية. عدة طرق مقترحة تتضمن عدد من المعاملات والمحددات التي تعتمد على مكان الكوكب الطريقة الجديدة المقترحة مستندة على الفتحة الدائرية للتلسكوب مع القوة الثالثة لدالة كاوس والتي تم ايجاد القيم المثالية لها واصبحت لها القدرة على تحسس الكواكب الخارجية لمسافة زاوية ($4\lambda/D$) ونسبة تباين (10^{-10}) وبالاضافة كونها سهلة ويمكن تطبيقها عملياً .

1-Introduction

Extrasolar planets could be detected by two ways. The first is indirect detection which include astrometery, radial velocity and microlensing. A large number of extrasolar planets have been discovered in the last fifteen years through indirect methods. Since the first planet around a sun-like star was discovered in 1995 [1], more than 1800 exoplanets in orbit around just over 1100 stars have

*Email: ali.talib@scbaghdad.edu.iq

been confirmed (for more details, see [2]). In this case, the planets are well separated from their parent stars, for example, the Fomalhaut is located just inside a large dust ring that surrounds the central star and is separated by 12.7 arcsecond [3].

The second is called direct imaging which involve observing the brightness distributions of an extrasolar planet that is located very close to its parent star. Many high contrast imaging techniques have been introduced during the last two decades. Apodized square aperture was suggested to detect a planet with angular separation of 4λ/D and at a contrast ratio ,C, of 10^{-10} [4]. It has been shown that an achromatic apodized pupil is suitable for imaging extrasolar planets could be obtained by reflection of an unapodized flat wavefront on two mirrors [5]. Spiderweb masks have been used to produce point spread function having annular dark zones [6]. Several different apodization approaches have been examined to achieve high contrast imaging based on the characterization of the pupil transmission function rather than masking the star in the image plane [7]. One-sided phase apodization technique was introduced to achieve high contrast imaging [8, 9]. Two-dimensional pupil apodization using arbitrary apertures to achieve high contrast detection was suggested by [10]. This optimized approach produces a 2-D shaped pupil with no simplifying geometric assumptions. Super Gaussian apodization functions in the telescope pupil plane or in the coronagraph Lyot plane has been introduced to improve the imaging contrast [11]. IDL package code for adaptive optics simulations is used to prepare a series of input point spread functions to achieve high contrast [12]. An apodized pupil lyot coronagraph in the context of exoplanet imaging with ground based optical telescopes has been examined. This combines an apodization in the pupil plane with a small lyot mask in the focal plane of the instrument [13]. A hybrid coronagraph configuration that uses a shaped pupil as the apodizing mask in a Lyot-style architecture is described [14]. This design is managed to surpasses 10^{-9} contrast starting from an angular separation of 2λ/D. A new solution for a podized pupil lyot coronagraph with segmented aperture telescopes to remove broadband diffraction light from a star with a contrast level 10^{-10}[15]. It is also important to see the review of small angle coronagraphs techniques by [16]. Despite the discoveries of some objects with planetary mass in the past few years [17-20], and the existence of many high contrast imaging techniques during the last two decade, observing exoplanet is still very challenging task because of the planet-star luminosity contrast ratio (10^{-6} for young giant planets and down to 10^{-8} to 10^{-10} for old giant and rocky planets). In addition, the angular separation between a planet and its parent star is quite small. Generally one needs a technique that is effective enough to capture the weak light photons of a very faint planet and simple to be practically implemented. The search for Earth-like planet requires a contrast level of ~ 10^{-10} and a separation of a few λ/D from the center of star. Imaging with optical telescope is not offering such observations. This is due to the fact that the aperture of the telescope creates a side loops attenuation pattern called Airy disc in which the brightness distributions of the planets are totally attenuated. The methods that described in the literatures that stated before are based on shaped pupil coronagraphs and apodization. They are more that one input parameter requirement techniques and they need to be optimized based on the location of the planet. The new simple technique offering circular aperture modified by third power Gaussian function and the standard deviation of this function is optimized and it is not depending on the location of the planet.

2-Mathematical Models:

The general complex pupil function of an optical telescope is given by [21]:

$$P(\zeta,\gamma) = A(\zeta,\gamma)e^{i\phi(\zeta,\gamma)} \quad (1)$$

where $A(\zeta,\gamma)$, $\phi(\zeta,\gamma)$ are the amplitude and the phase aberration of an optical system and (ζ,γ) are coordinates in the pupil function.

The function $i\phi(\zeta,\gamma)$ can be expanded using a Taylor series [22]:

$$e^{i\phi(\zeta,\gamma)} = 1 + i\phi - \phi^2/2 + ... \quad (2)$$

If there is no atmospheric turbulence and the telescope is free from any aberration then equation (1) becomes $P(\zeta,\gamma) = A(\zeta,\gamma)$ [23].

The pupil function of an optical telescope is a circular function of constant values, i.e.

$$A(\zeta,\gamma)=\begin{cases}1 \text{ if } r \le R\\ 0 \text{ otherwise}\end{cases} \quad (3)$$

where R *is* the radius of the optical telescope and r is given by:

$$r=\left[(\zeta-\zeta_c)^2+(\gamma-\gamma_c)^2\right]^{1/2} \quad (4)$$

(ζ_c,γ_c) is the coordinates of the central point of an array. The design of the pupil function is a vital element for direct imaging of extrasolar planets because it controls the amount of suppressing the wings of the point spread function (*psf*) owing to reveal the planet that buried under the diffraction rings of the star. We are looking for the requirements of an optical telescope that is being able to cancel starlight up to a 10^{10} factor and provide a good high angular resolution of the *psf* [24]. The apodization techniques have been suggested in order to overcome this kind of problem that faced us in direct imaging of extrasolar planets.

The new suggested approach is considering the pupil transmission function is obeying a Gaussian like shape function as given by:

$$G(\zeta,\gamma)=\begin{cases}\left[\exp\left(-\dfrac{r^2}{2\sigma^2}\right)\right]^{p} & \text{if } r \le R\\ 0 & \text{elsewhere}\end{cases} \quad (5)$$

where σ is the standard deviation and **p** <=1. If **p**=1, then the function becomes a typical Gaussian function.

To find the optical transfer function of an optical telescope, $T_\circ(u,v)$, we must consider the imaging of a point source (i.e. Dirac delta function point source). In this case, $T_\circ(u,v)$ becomes the autocorrelation of the pupil function,

$$T_\circ(u,v)=\int_{-\infty}^{\infty}\int_{-\infty}^{\infty}A(\zeta,\gamma)A^*(\zeta-\bar{\zeta},\gamma-\bar{\gamma})d\bar{\zeta}d\bar{\gamma} \quad (6)$$

The *psf* of any optical imaging system is the image of a point source. The electric field, E(x, y), in the image plane is the Fourier transform of the pupil function [25].

$$psf(x,y)=\left|E(x,y)\right|^2=\left|FT(A(\zeta,\gamma))\right|^2 \quad (7)$$

where *FT* denotes Fourier transform operator.

The optical transfer function of the extended object, $T(u,v)$ is written as,

$$T_\circ(u,v)=\int_{-\infty}^{\infty}\int_{-\infty}^{\infty}A(\zeta,\gamma)A^*(\zeta-\bar{\zeta},\gamma-\bar{\gamma})U(\zeta,\gamma)U^*(\zeta-\bar{\zeta},\gamma-\bar{\gamma})d\bar{\zeta}d\bar{\gamma} \quad (8)$$

where $U(\zeta,\gamma)$ is a complex wavefron of an object.

The image of a point source through a telescope-atmosphere system becomes:

$$psf(x,y)=\left|IFT(T(u,v))\right| \quad (9)$$

3 - Numerical Simulations

Computer simulations are carried out to demonstrate the efficiency of this new technique. First of all, let us start with a very simple example to identify the problem very clearly. $A(\zeta,\gamma)$ is taken to be a 2-D circular function of radius R, and of unity magnitude inside R and zero outside in an array of size N by N pixels according to eq.(3). The *psf* is then computed via eqs.(6 & 7) for different telescope diameters as shown in Figure-1.

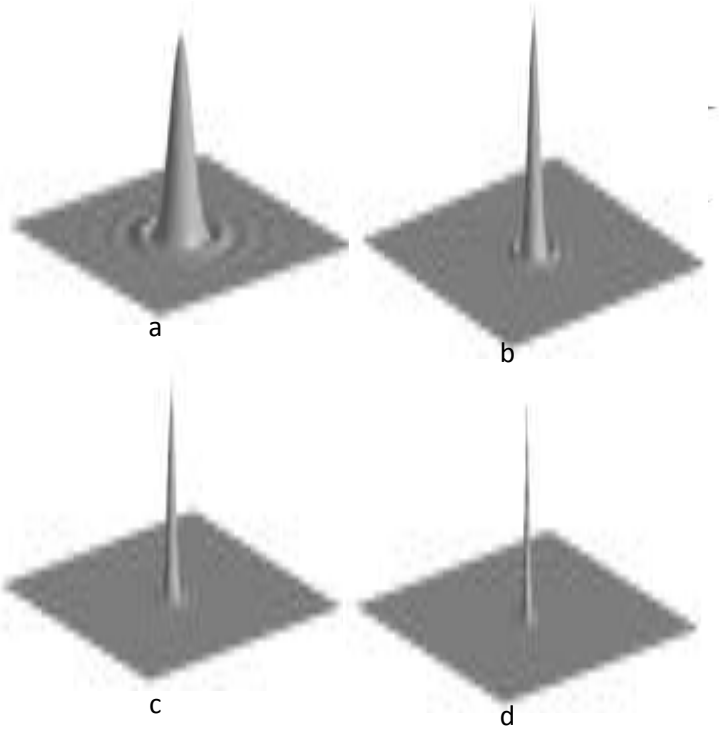

Figure 1- Surface plots of *psf* at different telescope diameters. a-D=50 pixels, b-2D, c- c=3D, d-5D.

These *psfs* are normalized to one at their maximum values, log10 (*psf*) are then computed and the central regions of the corresponding surface plots are shown in Figure-2. The 1-D central plots (the plot that started from the center of an array to its border) are also plotted and demonstrated in Figure-3

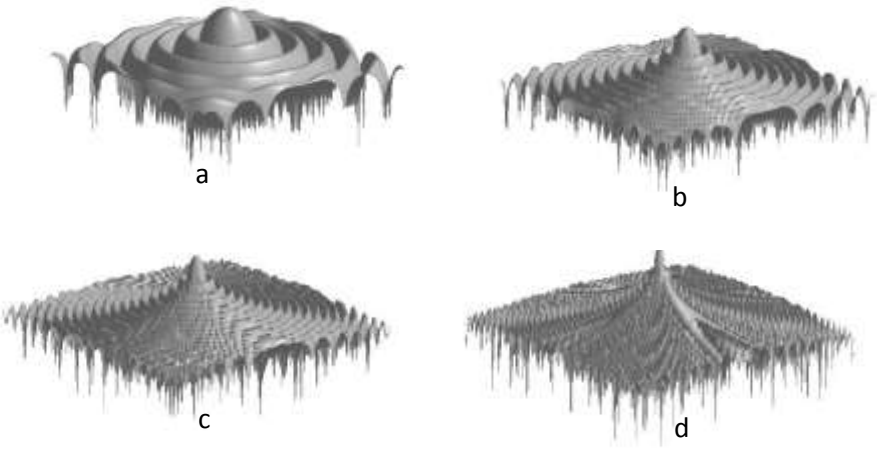

Figure 2- Surface plots of log10(*psf*) at different telescope diameters. a-D, b-2D, c- 3D, d-5D.

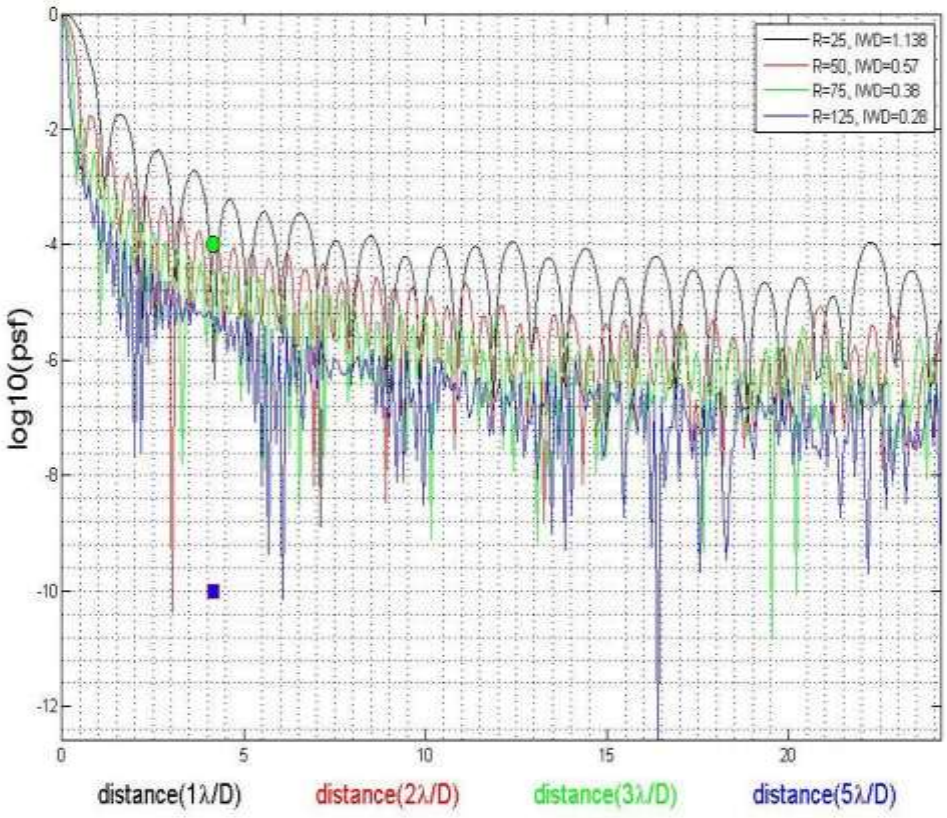

Figure 3- 1-D central plots through log10 (*psf*) for different aperture diameters.

The color labels on the x-axis indicating the values of angular distance in terms of λ/D relative to telescope diameter as shown in the legend box inside the figure.

The results indicate that as the radius of the telescope increases, the ripples beyond the central spike becomes sharper and the inner working distance, IWD (the distance from the central spike to the point at 1λ/D) becomes smaller. It should be pointed out here that the x-axis of the plot of Figure-3 illustrate four text labels according to the corresponding color plots. The green circle is a planet that located at 4λ/D (relative to scale D=50) for a black plot and 8λ/D (relative to D=100) for red plot and so on for the others. The green circle and blue square are at $C=10^{-4}$ and 10^{-10} respectively

It is now necessary to quantify the quality of these telescopes on observing a binary system with relative magnitude. The binary system (star and planet) are generated as,

$$Binary(x,y) = psfn(x,y) + C * psfn(x-\mathrm{d}, y-\mathrm{d}) \quad (10)$$

where *psfn*(x,y) is an image of a Dirac delta function observed by optical telescope and **d** is the shifted distance in terms of λ/D . *psfn*(x,y) and *psfn*(x-**d,**y-**d**) are normalized to one at their maximum values. The results of implementing eq.10 using different aperture diameters with **d**=4λ/D (relative to D=50) are shown in Figs.4 &5. The planet is hardly seen with D=50 and as D increases, the planet becomes clearly visible and wider and the star becomes sharper.

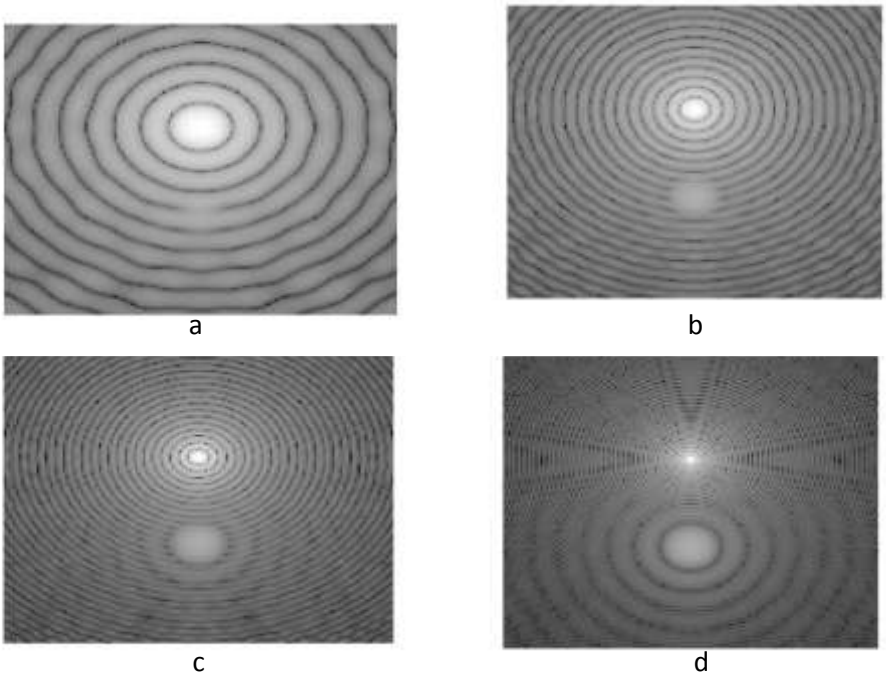

Figure 4 - Central images of star and planet at 4λ/ D (scale D) and $C=10^{-4}$ viewed through aperture diameters a-D, b-2D, c-3D, d-5D.

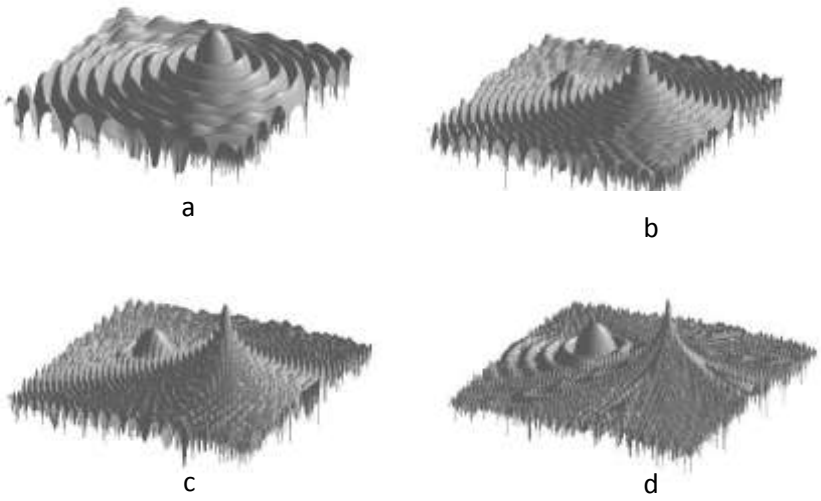

Figure 5 - Surface plots of Fig.(4) respectively.

The star is now taken to be much wider than a Dirac delta function and it is assumed to be a Gaussian function as given by:

$$star(x,y) = \exp(-\frac{(x^2+y^2)}{2\sigma^2}) \quad (11)$$

σ is set to 3 pixels which is reasonably wide compared with the planet that is taken as before as a Dirac delta function. This binary system is then convolved with the images of the Dirac delta function that observed by optical telescope of different diameters. The results are shown in Figures- 6 and 7.

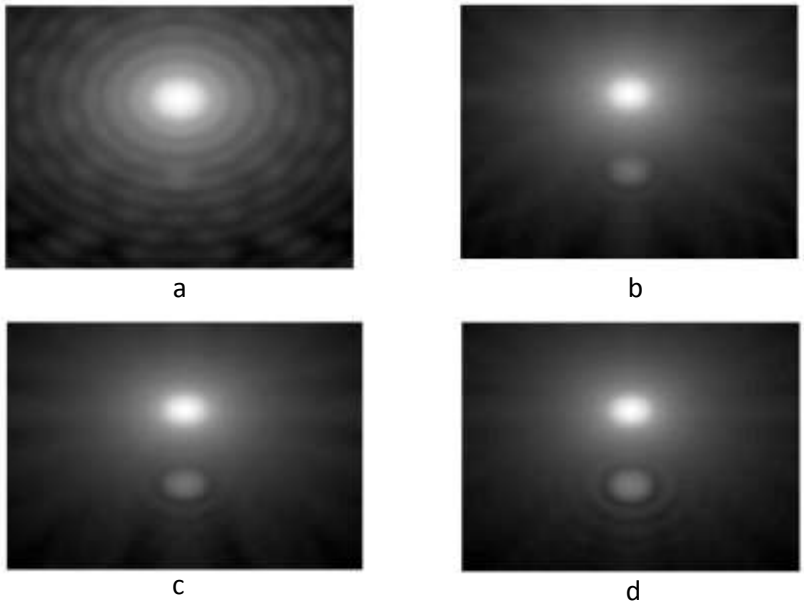

Figure 6 - Central images of star and planet at 4 λ /D (scale D) and C=10^{-4} viewed through a-D, b- 2D, c- 3D, d- 5D.

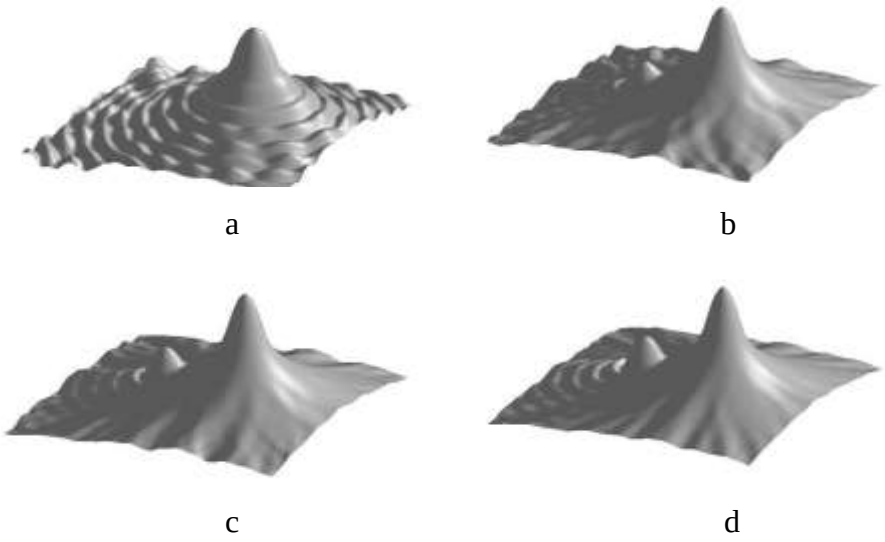

Figure 7- Surface plot of Figure- 6 respectively.

The new approach is implemented by generating a 2-D Gaussian shape function as stated in eq.(5). σ of this function is taken relative the telescope radius. For example, we vary σ from 10 pixels to 20 pixels with step size of 0.1 and **p** from 0 to one with step size of 0.1. The optimization criterion is based on obtaining a minimum IWD. The optimum values of σ and **p** are found to be 16.5 pixels and

0.3 respectively. Then we use the measure σ/D to be the controlling parameter for telescope diameter (i.e σ/D=0.132).

The 1-D central plots through the aperture magnitudes at different value of **p** for σ /D=0.132 are shown in Figure-8. For **p**=0, the aperture is a typical circular aperture with constant values as shown in black. As **p** increases, the aperture becomes sharper and at **p**=1, the function becomes a typical Gaussian function.

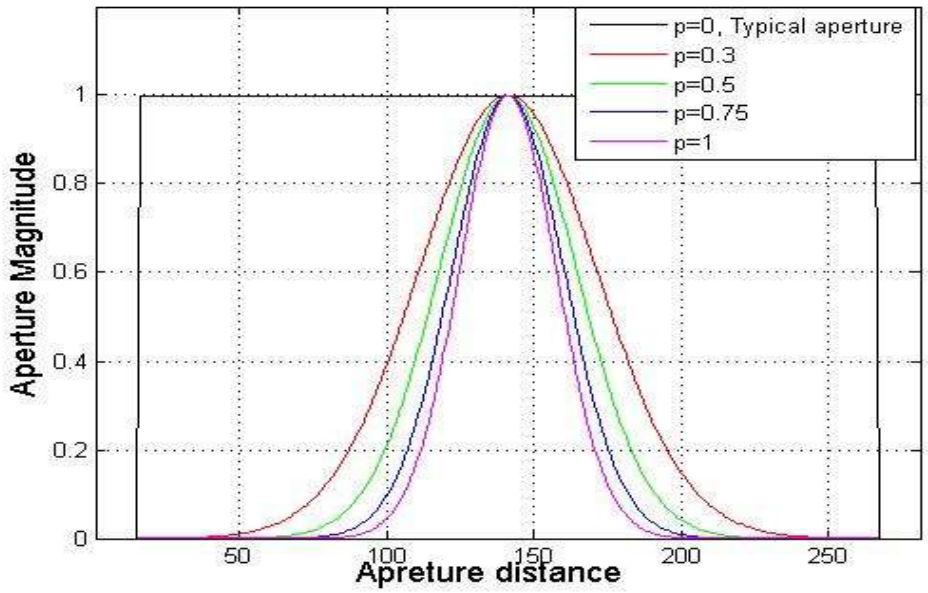

Figure 8 - Horizontal plots through the aperture magnitude for different values of **p**.

The log10(*psfs*) at a fixed σ/R=0.132 are then computed for different values of **p** and the corresponding 1-D central plots are shown in Figure-9. log10(*psf*) for the typical circular aperture are shown in black. The yellow circle is the location of the planet at 4λ/D and $C=10^{-10}$.
The results indicate that the IWD is just drops below 4λ/D at $C=10^{-10}$ for **p**=0.3. As **p** increases, the IWD becomes wider and at **p**=1, the IWD approaches 20λ/D. The outer working distance (the distance that started after IWD) dropping rapidly as **p** increases and reaches $C=10^{-27}$ for **p**=1 but on the expenses of IWD.

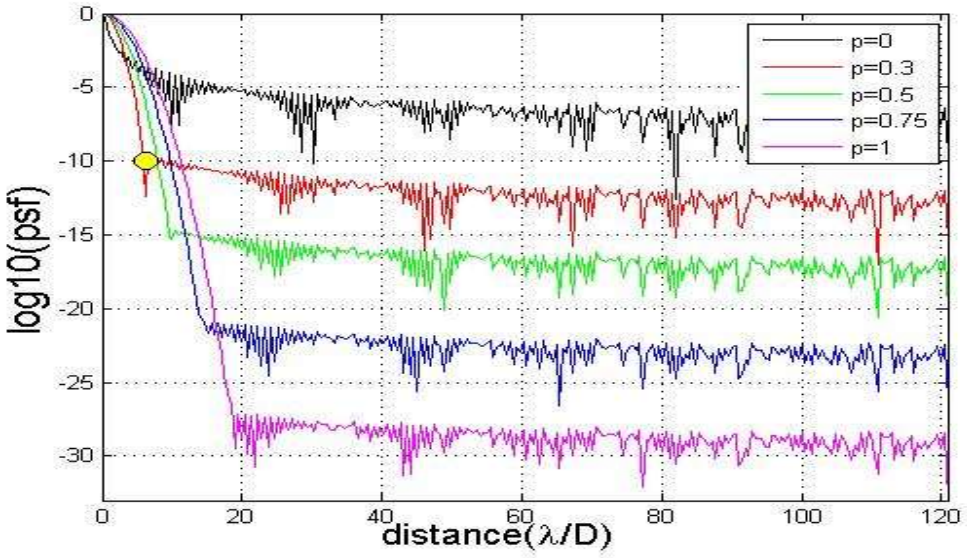

Figure 9 - log10 (*psfs*) as a function of distance in λ/D (relative to scale 5D) for different values of **p.**

The star and the planet are then generated via eq.(10). It should be pointed here that the *psfn*(x,*y*) is taken to be an image of a Dirac delta function observed by an optical telescope using the new aperture technique. The result using the optimized values of σ/R=0.132 and **p**=0.3 is shown in Figure-10.

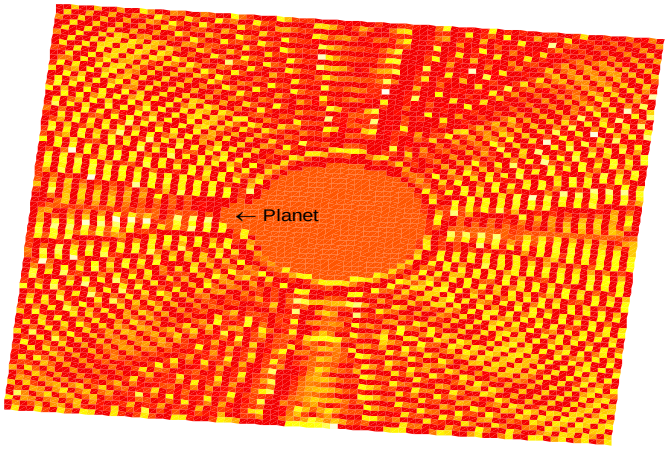

Figure 10 - Direct detection of a planet at **d**=4λ/D (scale 5D) and C=10^{-10}.

The new method is capable of detecting the planet as indicated in the arrow.

4 - Conclusions:

The central plots of the log10(*psfs*) indicate that using aperture diameters of D and 5D (i.e., five times bigger), there are no much declination in the side loops that created in the image of star especially within the IWD (i.e., less than 4 λ/D relative to the scale D). This demonstrates that using a very large ground-based optical telescope is not a step forwards to achieve high contrast imaging.

The optimized values of σ/D and **p** for the new approach that based on a minimum IWD criterion make the approach to be independent and not need any parameter to be adjusted and it is easy to be practically manufactured. For a planet that is located outside 4λ/D, and even at C <10^{-10}, it is recommended to use higher **p**.

References

1. Mayor, M., Queloz D.A. **1995**. Jupiter-Mass Companion to a Solar-Type Star. *Journal of Nature*, **378**: 355–359.
2. Rice, K. **2014**. The Detection and Characterization of Extrasolar Planets. *Challenges*, **5**: 296-223.
3. Kalas, P., Graham, J.R., Chiang, E. **2008**. Optical Images of an Extrasolar Planets 25 Light Years from Earth. *Journal of Science*, **322**, pp:1345.
4. Nisenson, P. and Papaliolios, C. **2001**. Detection of Earthlike Planets using Apodized Telescopes. *The Astrophysical J*, **548**: L201-L205.
5. Guyon, O. **2003**. Phase-Induced Amplitude Apodization of Telescope Pupils for Extrasolar Terrestrial Planet Imaging. *A & A Journal*, **404**: 379-387.
6. Vanderbei, R., Spergel, D. and Kasdin, N. **2003**. Circularly Symmetric Apodization via Starshaped Mask. arXiv:astro-ph/03050452v2.
7. Kasdin, N., Vanderbei, R., Spergel, D., and Littman, M. **2003**. Extrasolar Planet Finding via Optimal Apodized-Pupil and Shaped-Pupil Coronographs. *The Astrophysical Journal*, **582**: 1147-1161.
8. Yang, W. and Kostinski, A. **2004**. One – Sided Achromatic Phase Apodization for Imaging of Extrasolar Planets. *The Astrophysical Journal*, **605**: 892-901.
9. Weidong, Y. **2004**. Pupil Apodization for Achromatic Imaging of Extrasolar Planets. Ph.D. Thesis. Physics department, Michigan Technological University.
10. Carlotti, A., Vanderbei, R. and Kasdin, N. J. **2011**. Optimal Pupil Apodization for Arbitrary Apertures for High - Contrast Imaging. *Optics Express Journal*, **19**(27): 26796-26809.

11. Cagigas, M. A., Valle, P. J., and Cagigal, M. P. **2013**. Super-Gaussian Apodization in Ground Based Telescopes for High Contrast Coronograph Imaging. *Optics Express Journal*, **21**(10): 12744-12756
12. Mesa, D., Gratton, R., Berton, A., et al. **2011**. Simulations of Planet Detection with the SPHERE IFS. *A&A Journal* , **529**(A131): 1-11
13. Martinez, P. et.al. **2007**. Optimization of Apodized Pupil Lyot Coronograph for ELTs. *Astronomy and Astrophysics Journal*, **474**: 671-678.
14. Zimmerman, N. et al. **2016**. Shaped Pupil Lyot Coronographs: high Contrast solutions for Restricted Focal Planes. arXiv:1601.05121v1 [astro-ph.IM].
15. Mamadou, N. et al. **2016**. Apodized Pupil Lyot Coronographs for Arbitrary Apertures V hybrid Shaped Pupilo Designs for Imaging Earth-Like Planets with Future Space Observations. arXiv:1601.02614v1 [astro-ph.IM].
16. Dimitri, M. et al. **2012**. Review of Small-Angle Coronographic Techniques in the Wake of Ground-Based Second-Generation Adaptive Optics Systems. arXiv:1207.5481v1 [astro-ph.IM].
17. Marois, C., Macintosh, B., Barman, T., Zuckerman, B., Song, I., Patience, J., Lafreniere, D., Doyon, R. **2008**. Direct Imaging of Multiple Planets Orbiting the Star HR8799. *Journal of Science*, **322**: 1348-1352.
18. Lagrange, A. M., Bonnefoy, M., Chauvin, G., et al. **2010**. A Giant Planet Images in the Disk of the Young Star β Pictoris. *Journal of Science*, **329**: 57-59.
19. Chauvin, G., et al. **2012**. Deep Search for Companions to Probable Young Brown Dwarf-VLT/NACO Adaptive Optics Imaging using IR Wavefront Sensing. *A&A Journal*, **548**(A33):1-5.
20. Ginski, C., Mugrauer, M., Seeliger, M., et al. **2016**. A Lucky Imaging Multiplicity Study of Exoplanet Host Star II. *Accepted by MNRAS 2016*, January 6.
21. Fannjian, A. and Solana, K. **2005**. Propagation and Time Reversal of Wave Beams in Atmospheric Turbulence. *Society for Industrial and Applied Mathematics Journal*, **3**(3): 522-558.
22. Stribling, B., Welsh, B. and Roggemann, M. **1995**. Optical Propagation in Non- Kolmogorov Atmospheric Turbulence. *Proce. SPIE Journal*, **2471**, p: 22.
23. Golbraisk, E., Branover, H., Kopeika, N.S. and Zilberman, A. **2006**. Non – Kolmogorov Atmospheric Turbulence and Optical Signal Propagation. *Nonlin. Processes Geophys Journal*, **13**: 297-301.
24. Brummelear, J. **1996**. Modeling Atmospheric Wave Aberrations & Astronomical Instrumentations using the Polynomials of Zernike. *Journal of Optical Communications*, **132**: 329-342.
25. Fannjian, A. and Solana, K. **2005**. Propagation and Time Reversal of Wave Beams Atmospheric Turbulence. *Multiscale Model. Simul.,Society for industrial and Apllied Mathematics*, **3**(3): 522-558.